

couple nonlinearly to the oscillation. The mechanism may be visualized as a modulation of depolarization factors due to changes in shape of the highly conducting droplet. The resulting term in the Hamiltonian is proportional to BE_e^2 , where B is the amplitude of the oscillation and E_e is the external field. We expect to observe resonant absorption, or (in the presence of a static applied electric field in addition to the rf field) resonant second-harmonic generation, both at an applied frequency of $\omega/2$. Estimates of the amplitudes of these processes indicate that they could be observable. If so, the frequency of the resonance would provide information about γ via Eq. (8), and the width could, assuming small damping, reflect the size distribution of the electron-hole droplets.¹⁶

One of the authors (L.M.S.) would like to acknowledge a helpful conversation with G. W. Ford.

*Work supported by the National Science Foundation.

¹L. V. Keldysh, in *Proceedings of the Ninth International Conference on the Physics of Semiconductors, Moscow, U.S.S.R., 1968* (Nauka, Leningrad, U.S.S.R., 1968), p. 1303.

²V. E. Pokrovskii and K. I. Svistunova, *Pis'ma Zh.*

Eksp. Teor. Fiz. **13**, 297 (1971) [*JETP Lett.* **13**, 212 (1971)].

³Y. E. Pokrovskii, *Phys. Status Solidi (a)* **11**, 385 (1972), and references therein.

⁴C. Benôit à la Guillaume, M. Voos, and F. Salvan, *Phys. Rev. B* **5**, 3079 (1972), and **7**, 1723 (1973).

⁵J. C. Hensel, T. G. Phillips, and T. M. Rice, *Phys. Rev. Lett.* **30**, 227 (1973).

⁶P. H. Handel and C. Kittel, *Proc. Nat. Acad. Sci. U.S.A.* **68**, 3120 (1971).

⁷M. Combescot and P. Nozières, *J. Phys. C: Proc. Phys. Soc., London* **5**, 2369 (1972).

⁸W. F. Brinkman and T. M. Rice, *Phys. Rev. B* **7**, 1508 (1973).

⁹N. D. Lang and W. Kohn, *Phys. Rev. B* **1**, 4555 (1970).

¹⁰P. Hohenberg and W. Kohn, *Phys. Rev.* **136**, B864 (1964); L. J. Sham, in *Computational Methods in Band Theory*, edited by P. M. Marcus, J. F. Janak, and A. R. Williams (Plenum, New York, 1971).

¹¹This method is very similar to the technique used by K. A. Brueckner, J. R. Buchler, S. Jorna, and R. J. Lombard, *Phys. Rev.* **171**, 1188 (1968), to calculate the surface properties of a nucleus.

¹²J. R. Smith, S. C. Ying, and W. Kohn, *Phys. Rev. Lett.* **30**, 610 (1973).

¹³See, for example, A. B. Pippard, *Classical Thermodynamics* (Cambridge Univ. Press, Cambridge, England, 1966), p. 111.

Spin-Orbit Effect in the Si Valence Band*

Claudio Canali, Michele Costato, Gianpiero Ottaviani, and Lino Reggiani

Istituto di Fisica, Università di Modena, 41100 Modena, Italy

(Received 15 May 1973)

We report experimental evidence for a strong spin-orbit effect on the Si valence band. A theoretical evaluation of this effect on the hole mobility in the range of temperatures between 12 and 200°K is consistent with band-structure calculations, cyclotron-resonance measurements, and transport properties.

The small value of the spin-orbit energy in Si ($\Delta = 0.044$ eV¹) introduces a strong nonparabolicity of the two degenerate valence bands in a region near $\frac{1}{3}\Delta$. This effect, theoretically predicted by Dresselhaus, Kip, and Kittel² and by Kane,³ has not yet received full experimental evidence,⁴ mainly because of the great difficulties met in investigating regions of k space away from critical points.

The aim of this paper is to present new experimental data whose theoretical interpretation, in the light of the existing theories, seems to give unambiguously evidence for the nonparabolicity of the Si valence band. This evidence arises from an anomalous behavior which has been experimen-

tally found here in the temperature dependence of the hole mobility μ between 20 and 30°K (see Figs. 1 and 2). At these temperatures, provided the crystal is so perfect that only acoustic scattering is effective in determining the low-field transport properties, theory predicts a $T^{-3/2}$ temperature dependence for μ in spherical and parabolic bands. On the contrary, we have observed a strong deviation from this slope in the above temperature range, as is shown in Fig. 2. In Fig. 2(b) we have reported the behavior of $d(\ln\mu)/d(\ln T)$ as a function of T . Its peak can be correlated in detail to a band-structure effect which is expected to occur in the Si valence band because of its small spin-orbit energy. In fact a

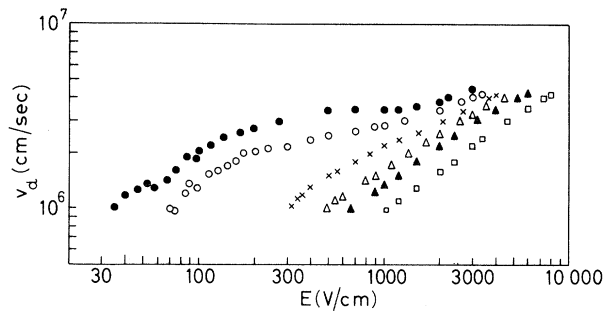


FIG. 1. Experimental field dependence of the drift velocity v_d at different temperatures for holes in Si. Closed circles, 12°K; open circles, 20°K; crosses, 30°K; open triangles, 38°K; closed triangles, 45°K; open squares, 60°K.

strong nonparabolicity of the upper valence band produces a sudden enhancement of the hole effective mass and, in turn, of the scattering rate. As a consequence, the hole mobility is expected to exhibit a slope steeper than $T^{-3/2}$ in the transient region.

The experimental apparatus was based on the time-of-flight technique coupled with the Università di Modena electron gun.⁵ Measurements of the drift velocity v_d of holes in Si have been performed in the range of temperatures between 12 and 200°K for different values of the applied electric field. The bath temperature was rigorously controlled within 0.5°K by a Ge resistance,⁶ while Joule heating was avoided by applying the electric field for short pulses lasting about 10^{-5} sec. The measurements were performed on different samples of hyperpure Si⁷ (room-temperature resistivity about $10^5 \Omega \text{ cm}$) along different crystallographic directions. The uncertainty of the measure is within 5%. Results are reported in Fig. 1 where v_d is given as a function of the applied electric field E for some temperatures of interest. The mobility as a function of temperature was obtained here by the ratio v_d/E at fixed values of v_d . Accordingly, curve 1 in Fig. 2(a) refers to $v_d = 1 \times 10^6$ cm/sec, and curves 2, 3, and 4 refer to 2, 3, and 4×10^6 cm/sec, respectively. Such a procedure was followed because v_d is not perfectly Ohmic at the lowest temperatures and fields attainable. As a consequence, our μ is field dependent even at the lowest v_d (curve 1). It is so understood that the family of curves reported in Fig. 2(a) running from 4 to 1 exhibit as a limit the behavior of the perfect Ohmic mobility, and that the effect here claimed is the more pronounced the more the mobility approaches the

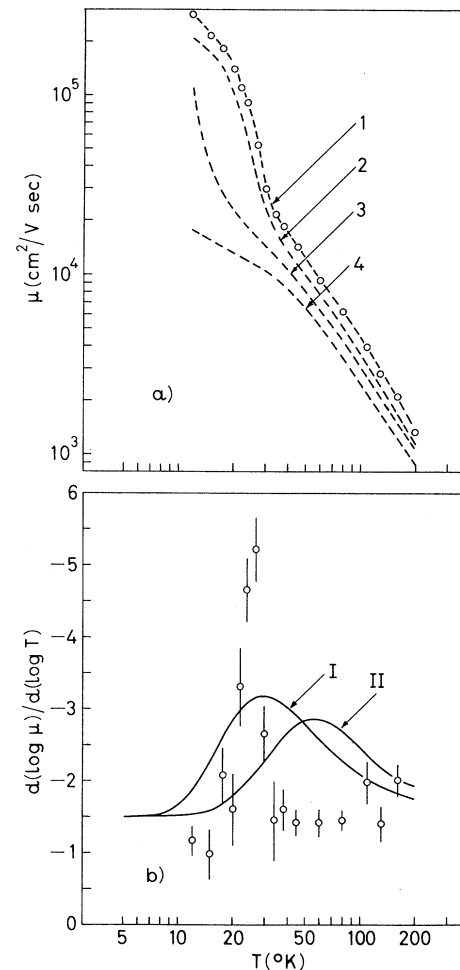


FIG. 2. (a) Experimental temperature dependence of the hole mobility μ in Si. Curves 1 to 4 refer to fixed values of the drift velocities ranging from 1 to 4×10^6 cm/sec, respectively. (b) Temperature dependence of $d(\ln \mu)/d(\ln T)$. Experimental points are deduced from curve 1 of (a). Curves I and II are the theoretical results according to choices I and II for the energy spectrum (see Fig. 3).

Ohmic limit.

To obtain a quantitative evaluation of this effect we have theoretically calculated the acoustic mobility of holes in Si making use of a band-structure model which accounts for the valence-band nonparabolicity. The energy spectrum of holes in Si for the $\langle 100 \rangle$, $\langle 110 \rangle$, and $\langle 111 \rangle$ crystallographic directions was evaluated by solving Eq. (30) of Ref. 3. For the inverse-mass band parameters A , B , and C we have used the values reported by Balslev and Lawaetz,⁸ which are the most up to date and generally accepted. The dispersion spectrum so obtained was here made isotropic by means of a weighted average of the

above solutions over the three directions.⁹ The results are reported in Fig. 3 by the shaded region for the heavy mass band E_{v1} , and dashed curve for the light mass band E_{v2} .¹⁰ The shaded region is due to the uncertainty in the values of B and C , where the latter brings the stronger contribution (see Table I). The band model has been defined according to

$$\begin{aligned}
 E_{v1} &= \hbar^2 k^2 / 2m_{10} \text{ for } 0 \leq E_{v1} < E_0, \\
 &= \hbar k / (2m_{10}\alpha)^{1/2} + E_\alpha \text{ for } E_0 \leq E_{v1} \leq E_1, \\
 &= \hbar^2 k^2 / 2m_{11} \text{ for } E_1 < E_{v1} < \infty,
 \end{aligned}
 \tag{1}$$

$$\begin{aligned}
 E_{v2} &= \hbar^2 k^2 / 2m_2; \\
 \alpha &= \left[\frac{(E_1 m_{11} / m_{10})^{1/2} - E_0^{1/2}}{E_1 - E_0} \right]^2, \\
 E_\alpha &= E_0 - (E_0 / \alpha)^{1/2}.
 \end{aligned}
 \tag{2}$$

The values of m_{10} and m_2 reported in Table I are those generally accepted at $\vec{k}=0$, while the choice of the parameters m_{11} , E_0 , and E_1 will fix the shape of the band model for E_{v1} away from $\vec{k}=0$. We have tested our model with two sets of values for E_0 and E_1 (choices I and II in Table I) and obtained the results shown by curves I and II in Fig. 3.

Assuming that acoustic scattering mechanism is only effective in the range of temperatures

here considered, and by using the deformation potential approach, we have evaluated the acoustic-scattering relaxation time for the case of the dispersion spectrum defined in Eq. (1).¹¹ We have here taken into account intraband as well as interband scattering considering the characteristic p -like symmetry of the valence-band wave functions.¹² In the relaxation-time approximation we have so obtained

$$\mu = \Xi T^{-3/2} \frac{H_1(1+K_1^{1/2}) / (1+K_1^{3/2}) + H_2 + H_3/K + H_4(1+K_2^{1/2}) / (1+K_2^{3/2})}{m_2 \{ 1 + 2\pi^{1/2} K_1^{3/2} [I_1 + 2(\alpha k_B T)^{3/2} I_2] + K^{3/2} I_3 \}},
 \tag{3}$$

$$H_1 = \int_0^{x_0} \exp(-x)x dx, \quad I_1 = \int_0^\infty \exp(-x)x^{1/2} dx,$$

$$H_2 = \int_{x_0}^{x_1} \exp(-x)x^{3/2} [x^{1/2} + 2(K_1 \alpha k_B T)^{3/2} (x - x_\alpha)^2]^{-1} dx, \quad I_2 = \int_{x_1}^\infty \exp(-x)(x - x_\alpha)^2 dx,$$

$$H_3 = \int_{x_0}^{x_1} \exp(-x)(x - x_\alpha)^2 x^{-1/2} [x^{3/2} + 2(K_1 \alpha k_B T)^{-3/2}]^{-1} dx, \quad I_3 = \int_{x_1}^\infty \exp(-x)x^{1/2} dx,$$

$$H_4 = \int_{x_1}^\infty \exp(-x)x dx,$$

TABLE I. Constants used for calculations: m_0 , free-electron mass; pw, present work.

	A	B	N^a	Δ (eV)	$\frac{m_{10}}{m_0}$	$\frac{m_{11}}{m_0}$	$\frac{m_2}{m_0}$	E_0/k_B (°K)	E_1/k_B (°K)
	-4.27	-0.63 ± 0.08	-8.75 ± 0.25	0.044	0.55	2.0	0.2	70 ^b	130 ^b
								100 ^c	360 ^c
Reference	8	8	8	1	pw	pw	pw	pw	pw

^a $C^2 = (N^2 - 9B^2)/3$.

^bChoice I.

^cChoice II.

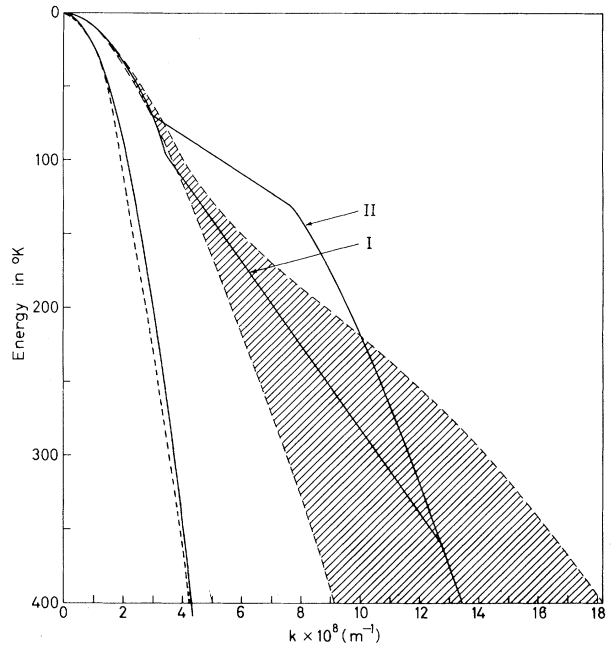


FIG. 3. Valence-band energy spectrum in Si. Shaded region and dashed curve represent results from $\vec{k} \cdot \vec{p}$ calculations for the heavy-hole mass band E_{v1} and light-hole mass band E_{v2} , respectively. Solid curves, present valence model. Curves I and II refer to choices I and II for E_0 and E_1 , respectively (see Table I).

where Ξ is a constant proportional to the coupling of acoustic modes, $K_1 = m_{10}/m_2$, $K_2 = m_{11}/m_2$, $K = m_{11}/m_{10}$, $x_i = E_i/k_B T$ ($i = 0, 1, \alpha$), and k_B is the Boltzmann constant.¹³

While the absolute value of μ depends on the value of Ξ , the effect of nonparabolicity can be correlated to the temperature dependence of $d(\ln\mu)/d(\ln T)$, the latter being independent from Ξ . It has been calculated by Tiersten¹⁴ that the inclusion of warping introduces a temperature-independent multiplicative factor in the acoustic mobility for a parabolic valence band. Accordingly the study of $d(\ln\mu)/d(\ln T)$ entitles us, in a first-order approximation, to neglect this effect. The study of this derivative permits us to overcome the systematic error due to the slight field dependence of the experimental mobility μ arising below 100°K. Theoretical results are compared with the experimental ones in Fig. 2(b), and the parameters used for calculations are reported in Table I. Curves *I* and *II* refer to choices I and II, respectively. We have found that, while *I* better approximates the band shape, it is *II* that better agrees with the experimental values of $d(\ln\mu)/d(\ln T)$. The better agreement between the experimental and theoretical amplitudes of the peak may be explained by taking into account explicitly the warping of the valence band. The broadening of the peak in the theoretical results with respect to experimental data has to be mainly ascribed to the slight field dependence of the experimental μ below 100°K. The tendency of μ to exhibit a steeper slope in the range of temperatures between 100 and 30°K is, in fact, masked by a carrier-heating effect which compelled the mobility to follow a nearly constant $T^{-3/2}$ slope.

In summarizing our finds we wish to point out that (1) the transport approach, in the limit of the present model, is treated rigorously. (2) Results in their essence are practically independent from the choice of the parameters which describe the band, provided the band model is consistent with the original $\vec{k} \cdot \vec{p}$ one. Consequently it is our belief that the theoretical picture unambiguously points out the effect of the spin-orbit interaction on the Si valence band.

As a final note supporting the present physical interpretation, an independent experimental investigation was performed, under identical conditions, on hyperpure Ge and has given no evidence of such an effect.¹⁵ This is in accord with

the larger value of the spin-orbit energy in Ge,¹ which should introduce nonparabolic effects at energies above 1000°K, well beyond the experimental reach.

In conclusion, we have for the first time found experimental evidence for the strong spin-orbit effect on the upper valence band of Si. Our theory has obtained the goal of gathering in a consistent manner (i) band-structure calculations, (ii) cyclotron-resonance data, and (iii) transport properties. A full comparison between experiment and theory in a larger range of temperatures, with the aim to improve the present understanding of the Si valence band away from $\vec{k} = 0$, is in progress.

The authors wish to thank Professor A. Alberigi Quaranta, Dr. C. Calandra, and Dr. C. Jacoboni for their helpful suggestions and critical comments.

*Work partially supported by the Consiglio Nazionale delle Ricerche.

¹P. Lawaetz, Phys. Rev. B **4**, 3460 (1971).

²G. Dresselhaus, A. F. Kip, and C. Kittel, Phys. Rev. **98**, 368 (1955).

³E. O. Kane, J. Phys. Chem. Solids **1**, 82 (1956).

⁴H. Miyazawa, K. Suzuki, and H. Maeda, Phys. Rev. **131**, 2442 (1963).

⁵C. Canali, G. Ottaviani, and A. Alberigi Quaranta, J. Phys. Chem. Solids **32**, 1707 (1971).

⁶Supplied by Scientific Instruments, Inc.

⁷Supplied by Wacker-Chemie GmbH.

⁸I. Balslev and P. Lawaetz, Phys. Lett. **19**, 6 (1965).

⁹For cubic crystals low field mobility reduces to a scalar quantity; thus the average we have introduced should give a reasonable approximation even if it masks the warped form of the equienergetic surfaces.

¹⁰The split-off band E_{v3} has been neglected because of its energy separation from E_{v1} and E_{v2} , and its small density of states which produces no detectable effects for the hole mobility in the range of temperatures considered.

¹¹Since acoustic scattering is here considered elastic and in the energy equipartition approximation, the acoustic-relaxation time τ is given by $\tau^{-1} = \int P(\vec{k}, \vec{k}') d^3k'$, $P(\vec{k}, \vec{k}') d^3k'$ being the usual scattering probability per unit time from \vec{k} into a state \vec{k}' .

¹²J. D. Wiley, Phys. Rev. B **4**, 2485 (1971).

¹³Some integrals can be analytically evaluated; and they are written in the form given for the sake of compactness.

¹⁴M. Tiersten, J. Phys. Chem. Solids **25**, 1151 (1964).

¹⁵G. Ottaviani, C. Canali, F. Nava, and J. Mayer, to be published.